

Tether Tension Variation of Tension Leg Platform (TLP) due to Random Waves

by

Mas Nazli Aziah Mohd Adnan

(7735)

Dissertation submitted in partial fulfillment of
the requirements for the
Bachelor of Engineering (Hons)
(Civil Engineering)

DECEMBER 2009

Universiti Teknologi PETRONAS

Bandar Seri Iskandar

31750 Tronoh

Perak Darul Ridzuan

CERTIFICATION OF APPROVAL

CERTIFICATION OF ORIGINALITY

**Tether Tension Variation of Tension Leg Platform (TLP) due to
Random Waves**

by

Mas Nazli Aziah Mohd Adnan

A project dissertation submitted to the

Civil Engineering Programme

Universiti Teknologi PETRONAS

in partial fulfilment of the requirement for the

BACHELOR OF ENGINEERING (Hons)

(CIVIL ENGINEERING)

Approved by,



(Prof. Dr. Kurian V. John)

UNIVERSITI TEKNOLOGI PETRONAS

TRONOH, PERAK

December 2009

CERTIFICATION OF ORIGINALITY

This is to certify that I am responsible for the work submitted in this project, that the original work is my own except as specified in the references and acknowledgements, and that the original work contained herein have not been undertaken or done by unspecified sources or persons.

Final

(MAS NAZLI AZIAH MOHD ADNAN)

ABSTRACT

Since petroleum exploration has shifted into deep water region, Tension Leg Platform (TLP) becomes one of the alternatives of floating platform. TLP is more economically feasible over jacket platform because its construction cost does not linearly increases as water depth increases. TLP allows movement in surge but not in heave. The presence of tethers components and the excess buoyancy of hull keep the TLP in tension. In this project, the response of TLP in surge, heave and pitch are studied. The study of tether performance is completed by analyzing the tension variation along the tether member. The dynamic analysis includes Pierson-Moskowitz Spectrum, Time Series and response of surge, heave and pitch when they are subjected to random waves. The result obtained from surge calculation is used to determine the tether tension variation. Then, graphs are plotted from the result obtained. Besides that, model testing was also conducted. The purpose of model testing is to observe the trend and the response of the structure when it is subjected to regular waves. From dynamic analysis and model testing activities, it is confirmed that TLP exhibits more response surge direction than heave due to the presence of tethers component. As conclusion, the TLP is kept floating and stable due to the presence of tether members which restrains its motion in heave direction.

ACKNOLEDGMENT

I would like to thank to various people involved in making this internship a success:

First and foremost, I would like to thank my FYP supervisor, Prof. Dr. Kurian V. John who found time in a very busy schedule to help me to understand more in this field. His passion for Civil Engineering has really inspired me. I am also deeply grateful for his advice, encouragement and patience throughout the past two semesters. The support he has given me as a valuable experience in a predominantly Malaysian environment has been greatly appreciated too.

Second, I would like to express my gratitude to my beloved mother, Rahkmas Bt Yunus for the support and encouragement upon the completion of this project.

Finally, I would like to express my gratitude to my entire colleagues especially Zafran Bin Sulaiman, Liyana Bahari and Aishah Radhiah Adanan who assisted me to complete the project.

ACKNOWLEDGMENT

I would like to thank to various people involved in making this internship a success:

First and foremost, I would like to thank my FYP supervisor, Prof. Dr. Kurian V. John who found time in a very busy schedule to help me to understand more in this field. His passion for Civil Engineering has really inspired me. I am also deeply grateful for his advice, encouragement and patience throughout the past two semesters. The support he has given me as a valuable experience in a predominantly Malaysian environment has been greatly appreciated too.

Second, I would like to express my gratitude to my beloved mother, Rahkmas Bt Yunus for the support and encouragement upon the completion of this project.

Finally, I would like to express my gratitude to my entire colleagues especially Zafran Bin Sulaiman, Liyana Bahari and Aishah Radhiah Adanan who assisted me to complete the project.

| | | |
|-------------------|--------------------------------------|-----------|
| 3.12 | Project Activities | 24 |
| 3.13 | Flow diagram of project activities | 25 |
| 3.14 | Gantt Chart | 26 |
| CHAPTER 4: | RESULTS AND DISCUSSION | 27 |
| 4.1 | Dynamic Analysis | 27 |
| 4.2 | Model Experimental Analysis. | 40 |
| CHAPTER 5: | CONCLUSION AND RECOMMENDATION | 42 |
| 5.1 | Conclusion | 42 |
| 5.2 | Recommendations | 43 |
| REFERENCES | | 44 |

LIST OF FIGURES

| | | |
|-------------|--|----|
| Figure 1.1 | Types of offshore platform | 1 |
| Figure 2.1 | Main components of Tension Leg Platform | 7 |
| Figure 2.2 | Type of Tension Leg Platform | 9 |
| Figure 2.3 | Schematic layout of Brutus TLP | 10 |
| Figure 2.4 | Degree of freedom of floating platform | 12 |
| Figure 2.5 | Surge force acting to the TLP | 13 |
| Figure 2.6 | Heave motion due to vertical forces | 14 |
| Figure 2.7 | Pitch moment on lateral axis | 14 |
| Figure 3.1 | Dimension of scaled down model | 21 |
| Figure 3.2 | Fabricated TLP Model | 22 |
| Figure 3.3 | TLP model in wave tank | 22 |
| Figure 3.4 | TLP model from the glass wall of the wave tank | 23 |
| Figure 4.1 | Graph of PM Spectrum | 28 |
| Figure 4.2 | Graph of Time Series | 29 |
| Figure 4.3 | Surge Motion Spectrum | 31 |
| Figure 4.4 | Surge Response | 31 |
| Figure 4.5 | Heave Motion Spectrum | 33 |
| Figure 4.6 | Heave Responses | 33 |
| Figure 4.7 | Pitch Motion Spectrum | 36 |
| Figure 4.8 | Pitch Response | 36 |
| Figure 4.9 | Tether Tension Spectrum | 38 |
| Figure 4.10 | Tether Tension Variation | 38 |
| Figure 4.11 | Tether Net Force, F_{net} | 39 |
| Figure 4.12 | The response of setup model in the wave tank | 40 |
| Figure 4.13 | Surge motion for model testing | 41 |

LIST OF TABLES

| | | |
|-----------|--|----|
| Table 2.1 | List of TLPs in the world | 6 |
| Table 2.2 | Summary of Brutus TLP | 11 |
| Table 2.3 | Wave parameters | 12 |
| Table 3.1 | Value of wave height and frequency for model testing | 23 |
| Table 4.1 | PM Spectrum | 27 |
| Table 4.2 | Preliminary data for surge calculation | 29 |
| Table 4.3 | Result of surge calculation | 30 |
| Table 4.4 | Preliminary data for heave calculation | 32 |
| Table 4.5 | Result of heave calculation | 32 |
| Table 4.6 | Preliminary data of pitch calculation | 34 |
| Table 4.7 | Result of pitch calculation | 35 |
| Table 4.8 | Calculation of tether tension variation | 37 |
| Table 4.6 | Result of surge motion of model testing | 40 |

ABBREVIATIONS & NOMENCLATURES

| | |
|---------------------|--|
| α | 0.0081 |
| π | 3.14159 |
| A_{col} | Cross-sectional area of column |
| $A_{pontoon}$ | Cross-sectional area of pontoon |
| C | Damping coefficient |
| C_m | Inertia coefficient |
| C_D | Drag coefficient |
| d | Water depth |
| D | Diameter |
| D_c | Column diameter |
| D_p | Pontoon diameter |
| E | <i>Modulus of elasticity</i> |
| f | Frequency |
| f_0 | Peak frequency |
| F_D | Drag force |
| F_I | Inertia force |
| F | Total force on structure |
| g | Gravity acceleration, 9.806 m/s ² |
| H_s | Significant wave height |
| $H(f)$ | Wave height at that frequency |
| k | Wave number |
| K | Stiffness |
| ΔL | Length increment |
| $L_{pontoon}$ | Length of pontoon |
| L | <i>Tether length</i> |
| m | <i>Mass of structure</i> |
| $M_{added, column}$ | Added mass of column |

| | |
|-----------------------------|----------------------------------|
| $M_{added, \text{pontoon}}$ | Added mass of pontoon |
| u | Horizontal particle velocity |
| u' | Horizontal particle acceleration |
| t | Time |
| T_n | Natural period |
| ω_0 | Peak frequency |
| ω_n | Natural frequency |
| s | Elevation from ocean floor |
| $S(f)$ | Energy density |
| ΔT | Increase in tension |
| x | Horizontal coordinate |
| ε | Random number |
| ρ | Density of water |
| Θ | $kx - \omega t$ |
| η | Wave profile or wave coordinate |

CHAPTER 1

INTRODUCTION

1.1 Background of Study

After the world has been reported about the depletion of petroleum resources, oil and gas industries have started to explore into deeper water area. Since Tension Leg Platforms (TLPs) is particularly well suited for deep water operation with water depth between 300 m to 1500 m, the demands for its construction has significantly increased.

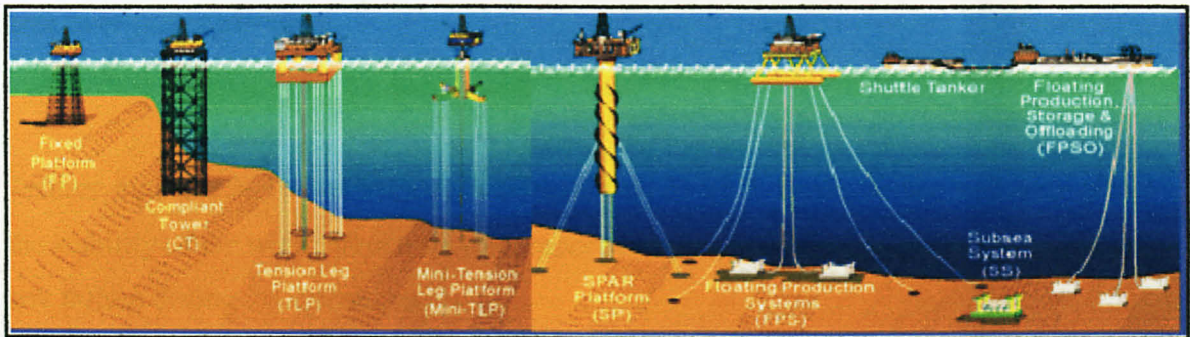


Figure 1.1: Types of offshore platform

A TLP is a compliant with free-floating offshore platform concept. Unlike fixed offshore platforms, compliant platforms respond to external effects by allowing limited motions. Tethers component controls the motions. TLP is compliant in the horizontal degrees of freedom, surge and sway. However, in the vertical degrees of freedom, a TLP is fixed.

The feature that distinguishes a TLP from other moored platform concepts is its reserve buoyancy. Since the buoyancy of a TLP exceeds its own weight, vertical moorings called “tendons” keep the TLP vertically stable and control heave motions.

1.2 Problem Statement

Tension Leg Platform (TLP) is one of the alternatives for deep water operation. Installation of TLP in deep water region is more favorable compared to other floating platform because TLP restrains the heave motion. The presence of tether components keeps the structure in tension and vertically stable in its position.

Construction cost is one of the important factors that should be considered in deciding type of offshore platform to be installed. However, TLP is not linearly increases as the water depth increases. Thus, TLP is economical feasible to be installed in deep water area over jacket platform.

Tethers member is one of important components in TLP. Since, tether will also affect the stability of the whole structure, it is important to properly design the tether to prevent any failure during the operation.

As the structure responses to the regular and random waves, the forces acting along the tether members will also change. The variation of forces along tether member will be mostly affected by surge response because theoretically, TLP exhibits more response in surge motion compared to heave motion. To confirm the theory, it is important to conduct motion analysis and complete this study.

Since Malaysia does not have installed any TLP yet, this is a good opportunity to study, analyze and feel the experience regarding TLP's structure in other famous area such as Gulf of Mexico.

1.3 Objectives and Scope of Study

1.3.1 The Objectives of Study

The study of the projects is done in order to achieve these two main objectives which are;

- To determine the motion of TLP in surge, heave and pitch direction when it is subjected to random waves by completing dynamic analysis of typical TLP. From the analysis, the motion in the interested direction is compared and further discussed.
- To work out the tension variation of tether components when it is subjected to regular and random waves. The calculation of tether tension variation will be conducted based on the result obtained from surge response.

1.3.2 Scopes of Study

In order to complete the study, detailed literature and journal related to tension leg platform were collected from Information Resources Centre Universiti Teknologi PETRONAS (IRCUTP) as well as from legal website.

To complete the study, the activities were divided into two parts which were dynamic analysis and model testing. Dynamic analysis was conducted based on Brutus TLP. The environment data such as significant wave height, maximum wave height and associated natural period was taken from PTS 20-0-73 of International Operation.

Energy distribution was determined first by using Pierson-Moskowitz Spectrum theory. From the energy distribution, the wave height at each frequency and the time series were then obtained. The horizontal forces acted on the structure are determined by using Morison Equation. These horizontal forces were used to determine response amplitude operator of motion response spectrum.

For the model testing, the dimension of Brutus TLP was scaled down with the ratio of 1:200 and fabricated. Then, the model was setup in the wave tank and tested by varying the wave height and wave frequency.

1.3.3 Relevancy of Project

Oil and gas industries contribute a large amount of monetary to Malaysia. It is very costly to operate and maintain the platforms by ourselves. To encourage cost saving and to minimal the risks, PETRONAS decided to employ specialist and competent consultant to operate it. By this, PETRONAS could create values to the world. This study is conducted as a preparation for future engineers, so that they are knowledgeable in this field.

CHAPTER 2

LITERATURE REVIEW

2.1 Tension Leg Platform (TLP)

Tension leg Platform (TLP) is a buoyant platform held in the place by a mooring system. The mooring system is a set of tension leg or tether attached to the platform and is anchored to the templates or foundation on the seabed.

Z. Demirebilek (1989) pointed out that “the feature that distinguishes a TLP from other moored platform concepts is its reserve buoyancy. Because the buoyancy of a TLP exceeds its weight, vertical moorings called tendons keep the TLP vertically stable and control heave motions.”

TLP is similar to conventional fixed platforms except that the platform is maintained on location through the use of moorings held in tension by the buoyancy of the hull. The tension leg mooring system permits for horizontal movement of surge and sway, but stiffly restrains vertical motion of heave. This advantageous causes TLP a popular choice for stability, such as in the hurricane-prone Gulf of Mexico.

The first TLP was installed in 1984 and used to develop the Hutton field in the North Sea with water depth of 148 meter. Hutton is the shallowest TLP being constructed and was run by Conoco. The deepest TLP is Magnolia TLP with the water depth of 1,425 meter which is located in Gulf of Mexico. Until today, 24 units of TLP were installed in the world.

Table 2.1 below is the summary of all TLPs in the world.

Table 2.1: List of TLPs in the world

| Tension Leg Platform | Year | Water Depth (m) |
|-----------------------------|-------------|------------------------|
| Hutton | 1984 | 147 |
| Oveng | 2007 | 271 |
| Snorre | 1992 | 335 |
| Heidrun | 1995 | 351 |
| El-Paso Prince | 2001 | 457 |
| Okume/Ebano | 2007 | 503 |
| ENI Morpeth | 1998 | 518 |
| Conoco Jolliet | 1989 | 536 |
| Chevron/Texaco Typhoon | 2001 | 639 |
| Matterhorn | 2003 | 859 |
| Auger | 1994 | 873 |
| Mars | 1996 | 896 |
| Brutus | 2001 | 910 |
| Ram-Powell | 1997 | 980 |
| Marlin | 1999 | 988 |
| Unocal West Seno 1 | 2003 | 1021 |
| Allegheny | 1999 | 1000 |
| Ursa | 1999 | 1200 |
| Kizomba A | 2004 | 1177 |
| Kizomba B | 2005 | 1177 |
| Neptune | 2007 | 1290 |
| Marco Polo | 2003 | 1311 |
| Shenzi | 2009 | 1311 |
| Magnolia | 2003 | 1432 |

2.2 Main components of TLP

A conventional TLP consists of topside, deck, column, pontoon, tethers and foundation templates (Figure 2.1)

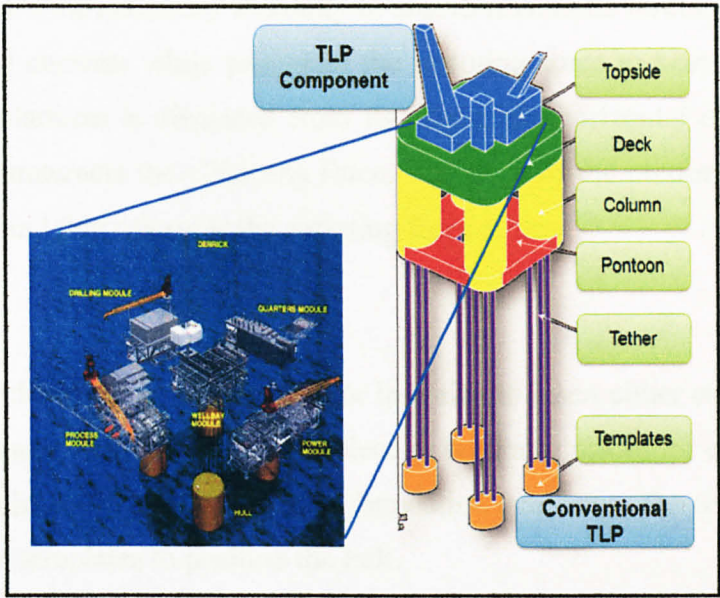


Figure 2.1: Main components of Tension Leg Platform

A supporting structure of a TLP consists of hull, tendons and foundation templates. The hull is a buoyant structure with a deck on its topside. The major functions of the deck are to control and support well, to separate gas, oil and non-transportable components in the raw product, to provide support for pumps, compressors, helideck as well as accommodation for operating and maintenance staff.

Each pontoon is connected to the columns to provide sufficient buoyancy and to maintain the stability of the platform even during storm condition. These columns are moored to the seabed through tendons or tension leg, and piled into the seabed with templates.

The excess buoyancy of TLP causes the structure to float. To keep the TLP in position, it requires tension legs or tendons to secure the structure on the seabed. Typical tethers are made from steel tube and it would be installed with as many as 12 tendons, 3 on each column.

The tether provides the necessary flexibility to absorb horizontal forces developed by the wind, waves and currents while providing the restoring force to keep the platform on station. As the platform is displaced from its origin, the horizontal component of the tether tension counteracts the offsetting force. The draft of the platform increases with limited distance and this enhances the restoring force effect.

A template provides a frame on the sea floor in which to insert either conductors or piles. A foundation template may be one single piece or separates pieces for each corner. Then the foundation piles are driven through the foundation templates. The tether will be fixed to the foundation templates to position the hull.

The total weight of TLPs includes all components that cause the structure to displace like topside, hull and weight of tendons.

- Personnel comfort and safety are increased.
- Problems with drilling equipment and process equipment that is sensitive to motion are minimized.

The MOSES TLP hull concept concentrates the column buoyancy closer to the center of the platform. Moses TLP consists of four rectangular columns of relatively smaller cross-sectional area with four large radial hull extensions at its base to support two tendon porches. Example of Moses TLP is Oveng TLP, Prince TLP and Marco Polo TLP.

2.4 Details of Typical TLP

In this study, Brutus TLP was selected for the analysis purpose. Figure 2.3 shows the schematic layout of Brutus TLP and its main components;

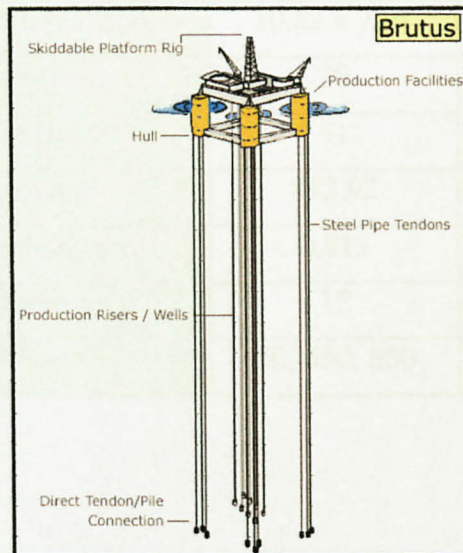


Figure 2.3: Schematic layout of Brutus TLP

Brutus is located 165 miles south-west of New Orleans. In April 1999, Shell (100% owners) announced plans to develop Brutus, to install a tension leg platform (TLP) on Green Canyon Block 158, in 910 meter of water.

The TLP facilities are designed to accommodate a peak gross production of approximately 100,000 barrels of oil per day and 300MMcf/d of gas. The TLP will be used as a hub for surrounding developments and thus, it is designed to handle an amount of gas greater than that required for the Brutus development (which is about 150MMcf/d of gas).

From the research and literature survey done, the summary of all required dimension of Brutus TLP are reported in Table 2.2.

Table 2.2: Summary of Brutus TLP

| Component | Dimension | Unit |
|-------------------|--------------|----------------|
| Water depth | 910 | m |
| Hull dimension | 81 x 81 | m ² |
| Pontoon dimension | 10.82 x 7.01 | m ² |
| Column diameter | 20 | m |
| Column height | 51 | m |
| Tendons length | 883.92 | m |
| Tendons diameter | 0.813 | m |
| No. of tendons | 12 | |
| Mass of TLP | 50, 650, 000 | kg |

Table 2.3 is the wave parameters that are used in the analysis. The parameters are taken from Petronas Technical Standard, Design of Fixed Offshore Structures (PTS 20-0-73). The dynamic analysis was conducted based on assumption that the Brutus TLP is installed in International Operation Area.

Table 2.3: Wave parameters

| | |
|--|--------|
| Individual maximum wave height, H_{\max} | 9.1 m |
| Associated wave period, T_{ass} | 10.6 s |
| Significant wave height, H_s | 4.9 m |

2.5 Degree of Freedom

In three dimensions, a rigid body has three translational displacements and three rotations with respect to x, y and z direction (Figure 2.4). The motions that a floating platform would experience are surge, heave, sway, roll, yaw and pitch. All those motion depend on the weight and buoyancy of the structure and environmental load that are encountered.

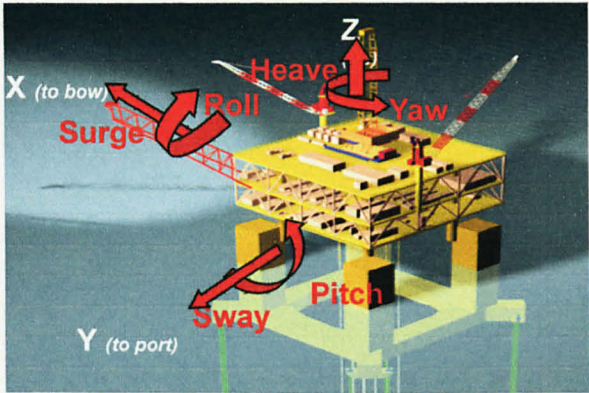


Figure 2.4: Degree of freedom of a floating platform

The basic motion is similar to that of an inverted pendulum. It is very flexible horizontally and rigid vertically. The effect of the tether is to eliminate vertical motion while permitting limited horizontal motion of the platform.

TLP is fixed by the tethers to the foundation and is kept in tension due to its excess buoyancy. Hence, the heave motion of TLP is almost negligible. However, TLP behaves like compliant platform and allows restrained movement with respect to the horizontal plane (surge).

Horizontal wave force that hit the structure would cause the surge motion. The draft keeps changing due to the tethers which restrain and push back the structure to its origin (Figure 2.5).

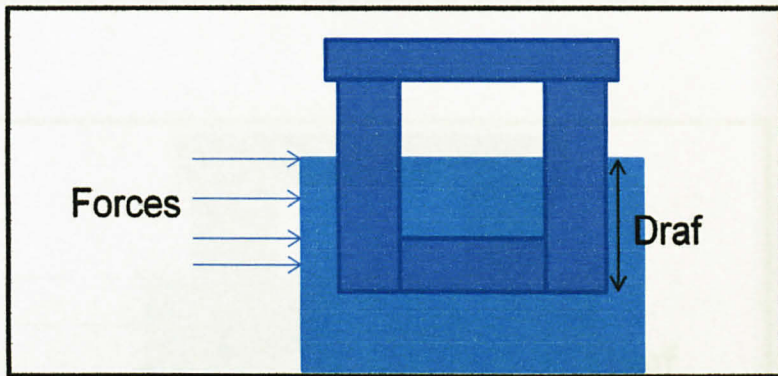


Figure 2.5: Surge Force Acting to the TLP

Meanwhile, heave motion is induced by the pressure and vertical forces that are acting on the bottom part of columns and pontoons. (Figure 2.6)

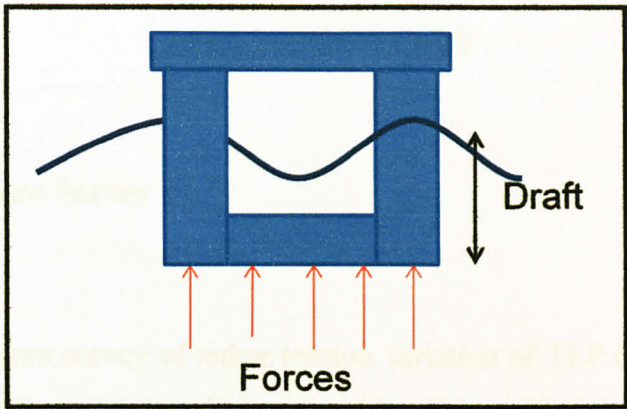


Figure 2.6: Heave motion due to vertical forces

Pitch is the moment of the structure. The force acting of the structure will be multiply with the length from the force acting to the center of gravity. (Figure 2.7)

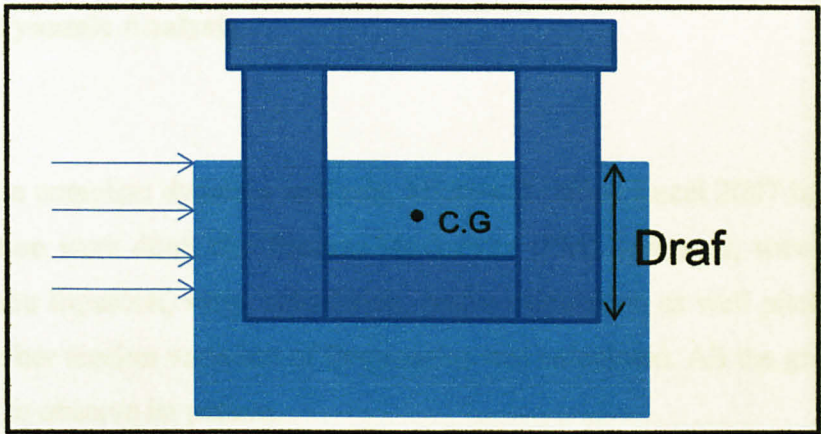


Figure 2.7: Pitch moment on lateral axis

CHAPTER 3

METHODOLOGY

3.1 Literature Survey

Research and literature survey of tether tension variation of TLP due to random waves had been completed by collecting all the related journals and articles that are available in Information Resources Centre Universiti Teknologi PETRONAS (IRCUTP) as well as from legal websites. The purpose of conducting literature survey is to collect and to gather all the data required for analysis. The data required like dimension of Brutus TLP and environment loads were also collected from the articles and journals gathered.

3.2 Dynamic Analysis

To work out a complete dynamic analysis, Microsoft Office Excel 2007 had been used. Few calculation were done like Pierson-Moskowitz (PM) Spectrum, wave profile/time series, Morison Equation, surge calculation, heave calculation as well pitch calculation. Lastly, the tether tension variation of frequencies was calculated. All the graphs required were plotted to observe its pattern.

3.3 Pierson-Moskowitz (PM) Spectrum

Pearson-Moskowitz (PM) has been extensively used by ocean engineers to plot the distribution of wave energy in the corresponding area.

The PM Spectrum model is written by;

$$S(f) = \frac{\alpha g^2}{2\pi^4} \times f^{-5} \times \exp \left[-1.25 \times \left(\frac{f}{f_0} \right)^4 \right] \quad (3.1)$$

$$\omega^2 = \frac{0.161g}{H_s} \quad (3.2)$$

$$f_0 = \frac{\omega}{2\pi} \quad (3.3)$$

A graph of energy distribution, $S(f)$ versus frequency, f was plotted. From the graph, the frequency of the most energy concentrated could be determined.

3.4 Time Series

From the PM Spectrum analysis, the wave height of particular frequency, $H(f)$ could be determined. At a frequency, f_1 with energy density of $S(f_1)$, the wave height and wave profile, $n(x, t)$ were calculated as follows;

$$H(f_1) = 2\sqrt{2 S(f_1)\Delta f} \quad (3.4)$$

$$n(x, t) = \sum_{n=1}^N \frac{H(n)}{2} \cos[k(n)x - 2\pi f(n)t + \varepsilon(n)] \quad (3.5)$$

Equation (3.5) shows that the random number $\varepsilon(n)$ is included in calculation to obtain random wave height.

3.5 Morison Equation

Since the wave flow is random and not steady, the flow around the column will be more complex than the steady flow. Morison equation combines the effects of water particle velocity and acceleration on the structure loading on the structure due to a regular wave. The total forces acted on the column surface are the summation of drag force, F_D and inertia force, F_I as computed below;

$$F = F_D + F_I \quad (3.6)$$

$$F_I = \rho \times C_m \times \frac{\pi}{4} \times D^2 \times u' \cdot ds \quad (3.7)$$

$$F_D = \rho \times C_D \times \frac{D}{2} \times |u| \times u \cdot ds \quad (3.8)$$

3.6 Surge Calculation

For surge calculation; the total buoyancy, total surge mass, total pretension, surge stiffness, natural period and wave frequency was first determined by using the following formula;

$$\text{Total Buoyancy} = (4 \times A_{col} \times \text{draft} + 4 \times A_{pontoon} \times L_p) \rho g \quad (3.9)$$

$$\text{Surge added mass} = M_{\text{added,column}} + M_{\text{added,pontoon}} \quad (3.10)$$

$$\text{Total surge mass} = \text{Mass of TLP} + \text{surge added mass} \quad (3.11)$$

$$\text{Total pretension} = \text{Total buoyancy} - \text{Mass of TLP} \quad (3.12)$$

$$\text{surge stiffness} = \frac{\text{Total Pretension}}{\text{Tether Length}} \quad (3.13)$$

$$\omega_n = \sqrt{\frac{\text{Surge Stiffness}}{\text{Total Added Mass}}} = \sqrt{\frac{k}{M}} \quad (3.14)$$

$$T_n = \frac{2\pi}{\omega} \quad (3.15)$$

When all the preliminary data above are calculated, the total forces acted on the structure are calculated by using Equation (3.6-3.8).

3.7 Heave Calculation

For heave calculation; total heave mass, heave stiffness, natural wave period, natural frequency, total pressure and total forces were also determined by using the following formula;

$$\text{Heave added mass} = M_{\text{added,column}} + M_{\text{added,pontoon}} \quad (3.16)$$

$$\text{mass}_{\text{column}} = 4 \times \rho \times \frac{\pi D_c^3}{12} \quad (3.17)$$

$$\text{mass}_{\text{pontoon}} = 4 \times \rho \times \frac{\pi D_p^2}{4} \times L_p \quad (3.18)$$

$$\text{Total heave mass} = \text{Mass of TLP} + \text{heave added mass} \quad (3.19)$$

$$\text{Stiffness}_{\text{Heave}} = \text{Tethers Stiffness} + \text{water plane area} \quad (3.20)$$

$$\text{Water plane area} = 4 \times \frac{\pi D^2}{4} \times \rho \quad (3.21)$$

$$\text{Pressure, } p = \rho g \times \frac{H}{2} \times \frac{\cosh ks}{\cosh kd} \times \cos \theta \quad (3.22)$$

$$\text{Force}_{\text{Heave}} = \text{Total pressure} \times \text{Area} \quad (3.23)$$

3.8 Pitch Calculation

Since pitch is the moment oscillated on the structure, the forces are multiplied with the length from the forces acted. The total mass and the moment produced were calculated by using the formula below;

$$\text{Pitch total mass} = \text{Surge total mass} \times \text{radius of gyration} \quad (3.24)$$

$$\text{Moment}_{\text{Pitch}} = \text{Force}_{\text{Surge}} \times \text{Distance to center of gravity} \quad (3.25)$$

3.9 Motion-Response Spectrum

A structure that is free to move in its motion will be critical near the resonance of the structure. Thus, it is very important to determine the overall response of the structure based on the design wave spectrum. The motion-response spectrum is determined by using the following formula;

$$S_{(f)} = RAO^2 \times S(f) \quad (3.26)$$

$$RAO = \left[\frac{F_i / \frac{H}{2}}{\sqrt{(K - m\omega^2)^2 + (C\omega)^2}} \right] \quad (3.27)$$

3.10 Tether Tension Variation of TLP

The tension along the length of tethers varies as the frequency changes. TLP is affected most by surge motion compared to heave. Thus, only the surge response is included for the calculation of tether tension variation.

To calculate the tether tension variation, the wave height, $H(f)$ and RAO of surge response is used to calculate the increment of tether length ΔL , tether stiffness, increase in tension and RAO of tether tension.

$$\Delta L = \frac{H(f) \times RAO_{surge}}{2} \quad (3.28)$$

$$k = \frac{EA}{L} \quad (3.29)$$

$$\text{Increase in Tension, } \Delta T = k \times L \quad (3.30)$$

$$RAO_{Tension} = \Delta T / H(f) \quad (3.31)$$

3.11 Model Experiment/Testing

A TLP model was designed and fabricated for experimental purpose. The model had been fabricated by using Perspex material. The TLP model was tested in the wave tank. The frequency and the wave height were set first before the testing was conducted.

3.11.1 Scaled Down Model

For model testing purpose and to suit with the budget provided, the actual dimension of selected TLP was scaled down with the ratio of 1:200. Figure 3.1 describes the details for model dimension;

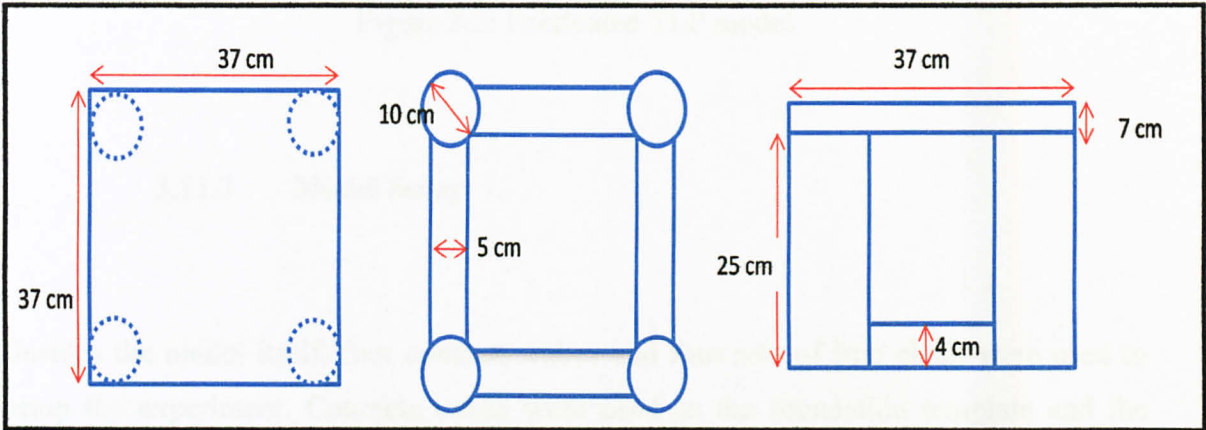


Figure 3.1: Dimension of scaled down model

3.11.2 Model Fabrication

The scaled model (Figure 3.2) was made from Perspex material. It was fabricated by Venus Distributor, situated in Taman Pengkalan Maju, Lahat, Ipoh. The cost of the model itself was RM355 with the weight of 2 kg. Perspex was chosen as the model material because it is lighter and easier to maintain.

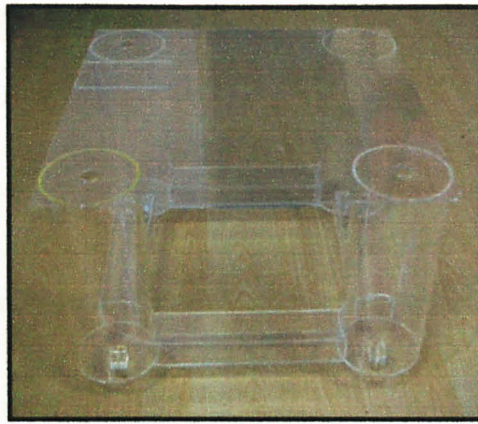
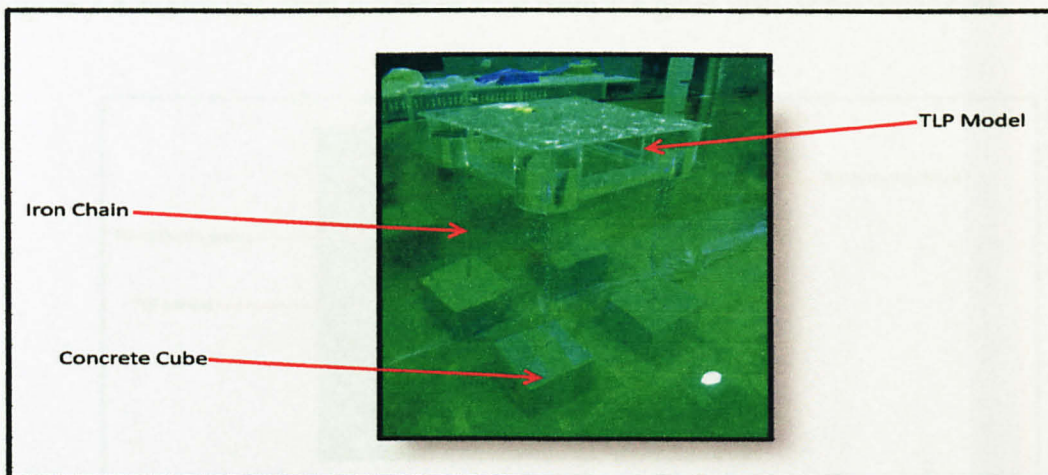


Figure 3.2: Fabricated TLP model

3.11.3 Model Setup

Besides the model itself, four concrete cubes and four sets of iron chain were used to setup the experiment. Concrete cubes were used as the foundation template and the tethers system was replaced by the iron chain. Each concrete cube has the dimension of 150 mm on each side. The length of each iron chain is 65 cm with the weight of 0.6 kg. Each set of iron chain was installed at each bottom of the column to connect the model with the concrete cube. To reduce its motion, weights were attached at the bottom of the column. Figure 3.3 is the TLP model that had been setup in the wave tank.



Figure

3.3: TLP model in wave tank

3.11.4 Experiment Procedure

After the model had been setup in the wave tank, the water depth was increased up to 1 m. A transparent graph was attached on the glass wall of the wave tank to read and measure the model motion. Besides that, video camera was setup to record the motion of model.

The model was tested by changing the value of the wave height, H and wave frequency, f . The surge and heave motion were observed and calculated. Table 3.1 is the value of H and f that has been used.

Table 3.1: Value of wave height and frequency for model testing

| | Wave Height, H (m) | Wave Frequency, f (Hz) |
|---|-------------------------|-----------------------------|
| 1 | 0.1 | 1 |
| 2 | 0.05 | 0.5 |
| 3 | 0.05 | 1 |

Figure 3.4 shows the setup model of TLP from the glass wall of the wave tank.

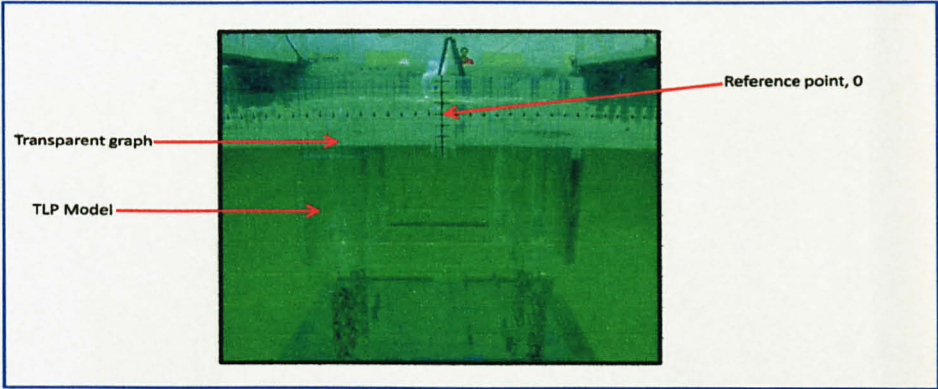
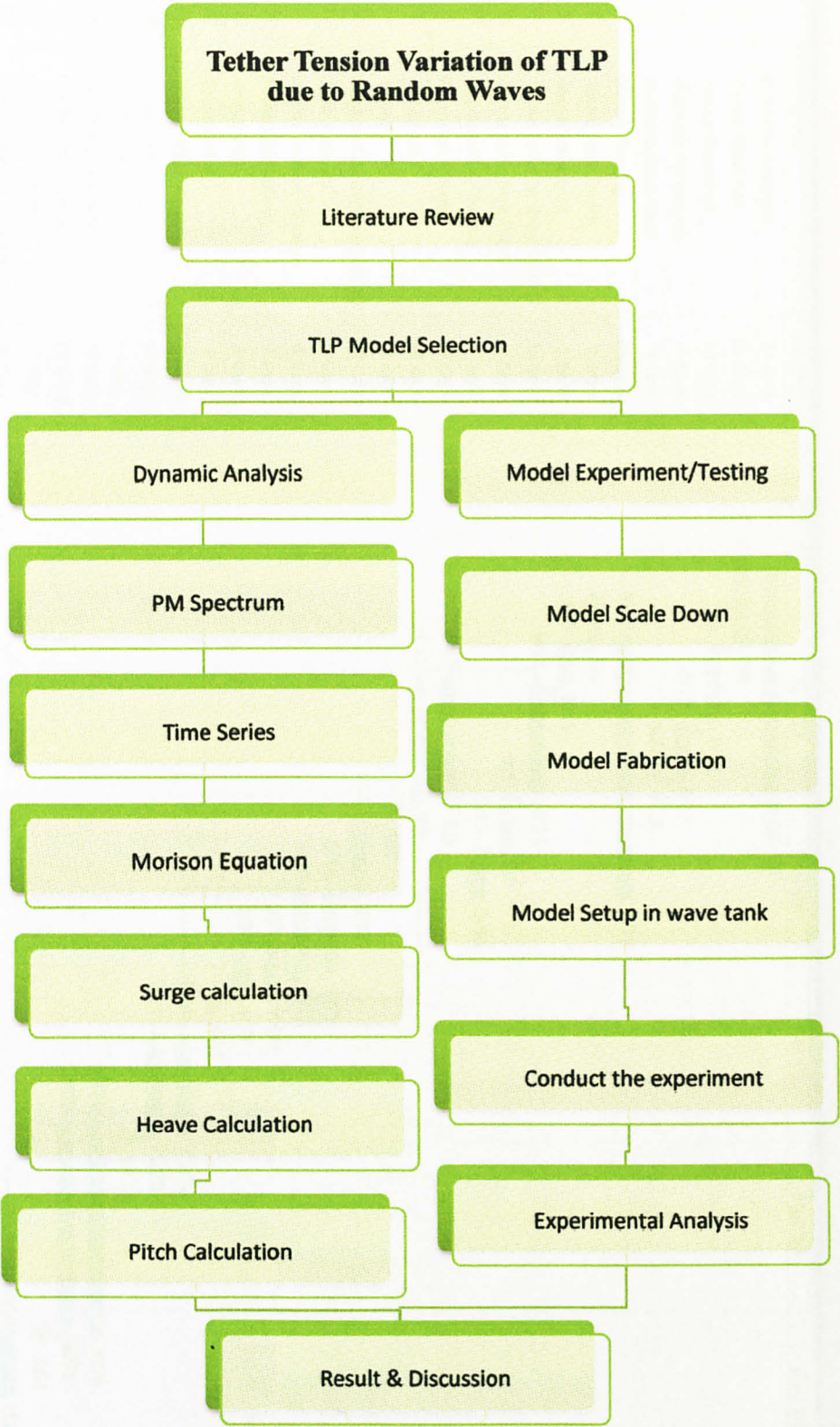


Figure 3.4: TLP model from the glass wall of the wave tank

3.12 Project Activities

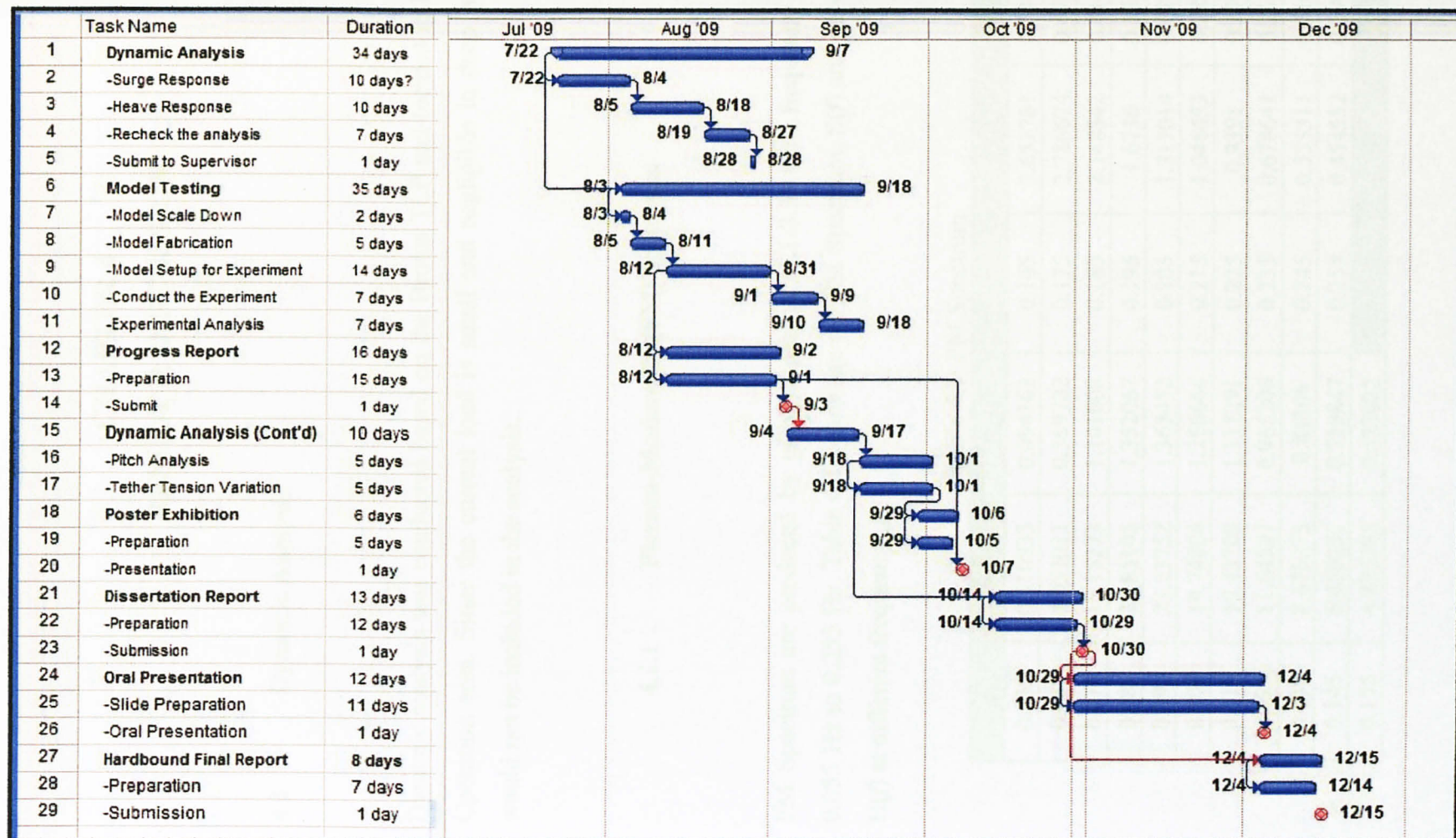
All the activities had been completed as per planned in the schedule. The literature review, surge and heave calculation were completed before the mid semester break. Model testing were conducted just after the mid semester break, followed by analysis of pitch and tether tension variation.

3.13 Flow diagram of project activities



3.14

Gantt Chart



CHAPTER 4

RESULT & DISCUSSION

4.1 Dynamic Analysis

Dynamic analysis was conducted based on the Brutus TLP and located in International Operation area. Since the current load is small and negligible in deep water area, it would not be included in the analysis.

4.1.1 Pierson-Moskowitz (PM) Spectrum

PM Spectrum are produced by using Equation (3.1-3.3) with frequency varies from 0.055 Hz to 0.255 Hz. Table 4.1 below are the PM Spectrum, $S(f)$ and its wave height, $H(f)$ at different frequency, f .

Table 4.1: PM Spectrum

| f | $S(f)$ | $H(f)$ | f | $S(f)$ | $H(f)$ |
|-------|----------|----------|-------|----------|----------|
| 0.055 | 0.110833 | 0.094163 | 0.165 | 3.652781 | 0.540576 |
| 0.065 | 4.057011 | 0.569702 | 0.175 | 2.786674 | 0.472159 |
| 0.075 | 15.15273 | 1.101008 | 0.185 | 2.148342 | 0.414569 |
| 0.085 | 22.85105 | 1.352067 | 0.195 | 1.6736 | 0.365907 |
| 0.095 | 23.23752 | 1.363452 | 0.205 | 1.317014 | 0.324594 |
| 0.105 | 19.74006 | 1.256664 | 0.215 | 1.046453 | 0.289338 |
| 0.115 | 15.43709 | 1.111291 | 0.225 | 0.8391 | 0.259091 |
| 0.125 | 11.64527 | 0.965206 | 0.235 | 0.678641 | 0.233005 |
| 0.135 | 8.675273 | 0.83308 | 0.245 | 0.553311 | 0.210392 |
| 0.145 | 6.459257 | 0.718847 | 0.255 | 0.454552 | 0.190694 |
| 0.155 | 4.836385 | 0.622022 | | | |

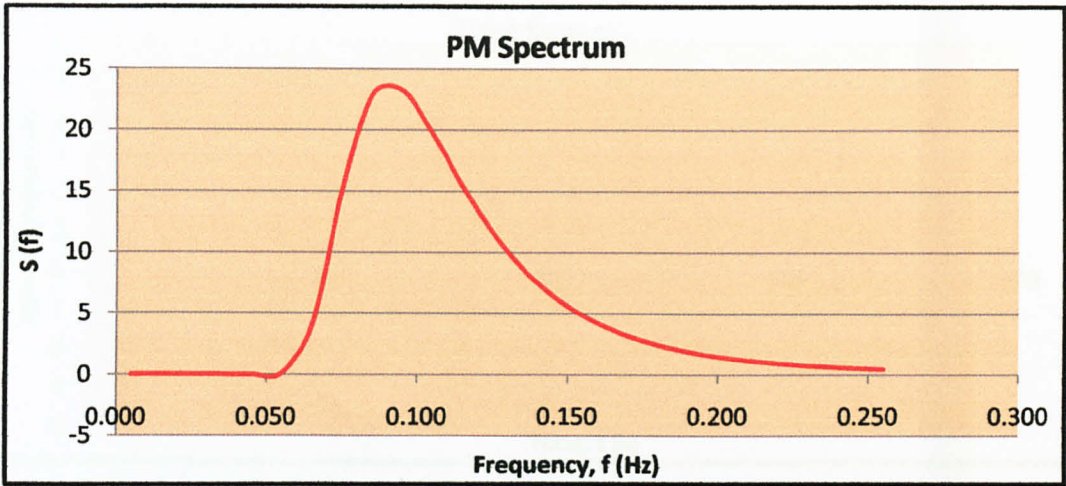


Figure 4.1: Graph of PM Spectrum

From Figure 4.1, the energy density, $S(f)$ for this wave profile shows that the maximum value for this wave is 23.24 m^2 . Most of the energy density concentrates on the frequency between 0.065 Hz to 0.175 Hz.

4.1.2 Time Series

After the PM Spectrum was plotted and the wave height at each frequency was determined, the wave profile was calculated by using equation (3.4-3.5). Figure 4.2 is the plotted wave profile;

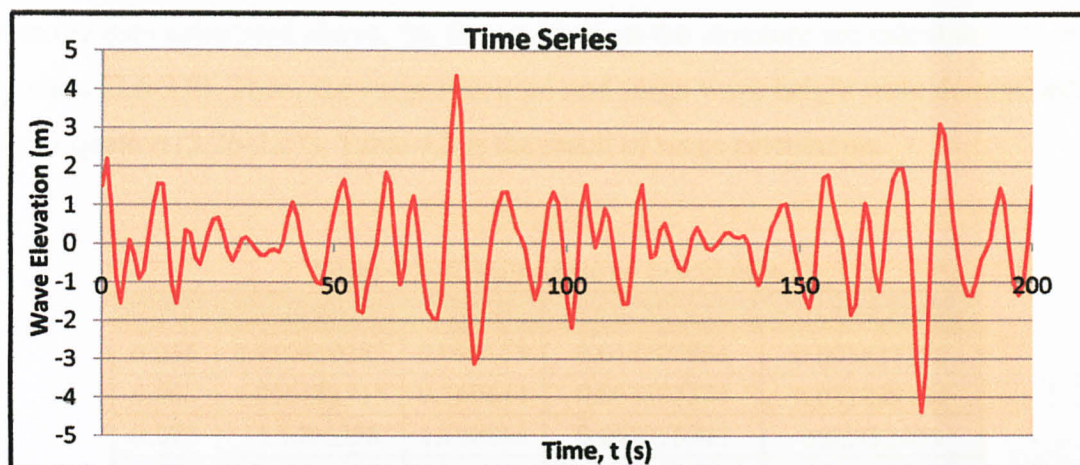


Figure 4.2: Graph of Time Series

The wave profile shows non linear excursion due to the presence of random waves. The waves are in the range of ± 5 m with the maximum wave elevation of 4.38 meter.

4.1.3 Surge Response

The total buoyancy, total mass, surge stiffness, natural period and natural frequency were calculated by using Equation (3.9-3.15). The result of the calculation was summarized in the Table 4.2;

Table 4.2: Preliminary data for surge calculation

| | | |
|-----------------------------|-------------|-------|
| Total buoyancy | 3895.6162 | MN |
| Surge added mass | 25756056.83 | kg |
| Total Surge Mass | 76406056.83 | kg |
| Total Pretension | 3398.8917 | MN |
| Surge stiffness | 3.8452 | MN/m |
| Natural period. T_n | 28.0080 | s |
| Natural frequency, ω | 0.2243 | rad/s |

From the data calculated above, the forces acted on the structure are calculated by using Equation (3.6-3.8). Then, the surge spectrum and surge wave height were determined by using Equation (3.26-3.27). Table 4.3 is the result of surge calculation.

Table 4.3: Result of surge calculation

| f | $S(f)$ | $H(f)$ | $RAO^2.S(f)$ | Surge $H(f)$ |
|-------|-------------|----------|--------------|--------------|
| 0.055 | 0.110810282 | 0.094153 | 0.014306984 | 0.033831328 |
| 0.065 | 4.056183315 | 0.569644 | 0.064593388 | 0.071885124 |
| 0.075 | 15.1496356 | 1.100895 | 0.095755742 | 0.08752405 |
| 0.085 | 22.84639419 | 1.351929 | 0.050359602 | 0.063472578 |
| 0.095 | 23.23278303 | 1.363313 | 0.159550481 | 0.112978044 |
| 0.105 | 19.73603579 | 1.256536 | 1.199128148 | 0.309726092 |
| 0.115 | 15.433941 | 1.111177 | 0.665566003 | 0.230749388 |
| 0.125 | 11.64290002 | 0.965107 | 1.10509633 | 0.297334334 |
| 0.135 | 8.673503581 | 0.832995 | 0.095047643 | 0.087199836 |
| 0.145 | 6.457939374 | 0.718773 | 0.020590193 | 0.040585902 |
| 0.155 | 4.835399168 | 0.621958 | 0.003020387 | 0.015544482 |
| 0.165 | 3.652036303 | 0.540521 | 0.103376187 | 0.090940062 |
| 0.175 | 2.786105256 | 0.472111 | 0.107331725 | 0.092663574 |
| 0.185 | 2.147903488 | 0.414527 | 0.000900686 | 0.008488516 |
| 0.195 | 1.673258804 | 0.36587 | 0.000319526 | 0.005055893 |
| 0.205 | 1.316745486 | 0.324561 | 0.004650911 | 0.01928919 |
| 0.215 | 1.046239416 | 0.289308 | 0.022230805 | 0.042171844 |
| 0.225 | 0.838928827 | 0.259064 | 0.00550599 | 0.020987596 |
| 0.235 | 0.678502355 | 0.232981 | 1.04723E-05 | 0.000915304 |
| 0.245 | 0.553198522 | 0.210371 | 0.002651952 | 0.014565581 |
| 0.255 | 0.454459177 | 0.190674 | 2.81606E-10 | 4.74642E-06 |

From the result obtained above; the graph of surge motion spectrum. Then, the surge response was plotted.

Figure 4.3 below is the surge spectrum. The energy spectrum is fluctuated with most of energy concentrated at the frequency of 0.100 Hz to 0.135 Hz.

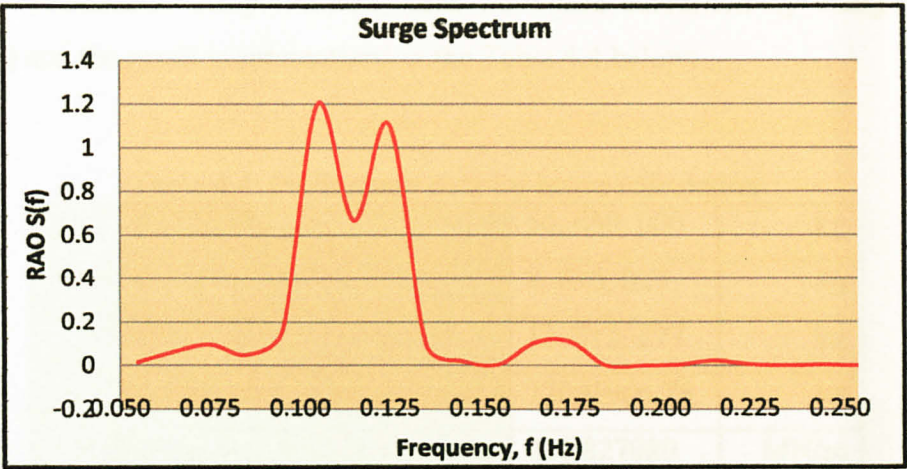


Figure 4.3: Surge Motion Spectrum

Lastly, the graph of surge responses is plotted (Figure 4.4). Surge responses provide the maximum wave height at the area of designed structure. From the analysis conducted, the maximum surge elevation is 0.52 m.

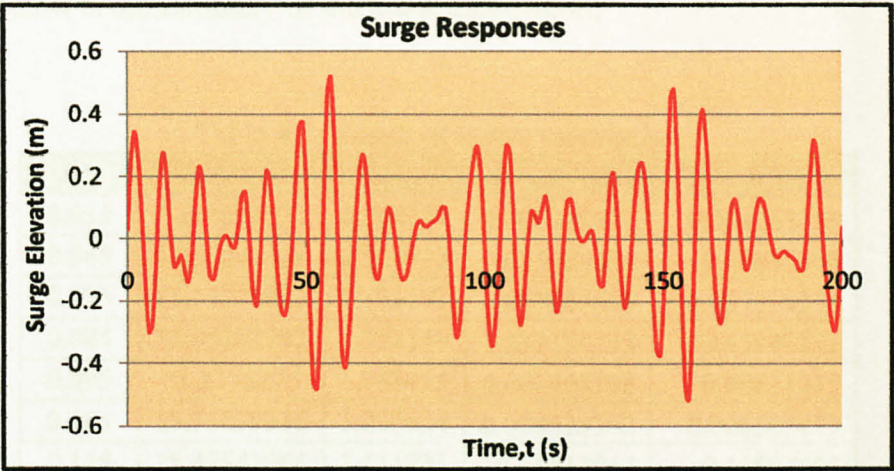


Figure 4.4: Surge Response

4.1.4 Heave Responses

For heave calculation, the preliminary data were first calculated by using Equation (3.16-3.21) and the result is summarized in the Table 4.4 below;

Table 4.4: Preliminary data for heave calculation

| | | |
|-------------------------------|--------------|---------|
| Mass of TLP | 50, 650, 000 | kg |
| Added mass heave for columns | 8, 630, 027 | kg |
| Added mass heave for pontoons | 12, 812, 277 | kg |
| Total mass heave | 72091906.78 | kg |
| Heave stiffness | 221.827080 | MN/m |
| Heave angular wave frequency | 1.75 | rad/sec |
| Heave Natural period | 3.58 | sec |

From the preliminary data above, the total forces acted vertically on the columns and pontoons components are calculated by using Equation (3.22-3.23). The heave motion spectrum and heave response were then calculated by using Equation (3.26 – 3.27). Table 4.5 below is the summary of the heave calculation;

Table 4.5: Result of heave calculation

| f | $S(f)$ | $H(f)$ | $RAO^2.S(f)$ | Heave $H(f)$ |
|-------|-------------|----------|--------------|--------------|
| 0.055 | 0.111016121 | 0.094241 | 0.000283671 | 0.004763789 |
| 0.065 | 4.060044004 | 0.569915 | 0.055034804 | 0.06635348 |
| 0.075 | 15.15776892 | 1.101191 | 0.017867606 | 0.037807519 |
| 0.085 | 22.85382792 | 1.352149 | 0.231190215 | 0.135997122 |
| 0.095 | 23.2376275 | 1.363455 | 0.000498198 | 0.00631315 |
| 0.105 | 19.73879336 | 1.256624 | 0.000528202 | 0.006500473 |
| 0.115 | 15.43543965 | 1.111231 | 0.16813064 | 0.11597608 |
| 0.125 | 11.64370992 | 0.965141 | 0.000855303 | 0.008271896 |
| 0.135 | 8.673947052 | 0.833016 | 6.00737E-08 | 6.93246E-05 |
| 0.145 | 6.458187473 | 0.718787 | 9.51472E-05 | 0.002758944 |
| 0.155 | 4.835541436 | 0.621967 | 5.01238E-06 | 0.000633238 |

| | | | | |
|-------|-------------|----------|-------------|-------------|
| 0.165 | 3.652119978 | 0.540527 | 8.8383E-05 | 0.002659068 |
| 0.175 | 2.786155703 | 0.472115 | 1.00123E-05 | 0.000894977 |
| 0.185 | 2.147934628 | 0.41453 | 6.14023E-06 | 0.00070087 |
| 0.195 | 1.673278457 | 0.365872 | 1.70871E-08 | 3.69726E-05 |
| 0.205 | 1.316758148 | 0.324562 | 6.9059E-07 | 0.000235047 |
| 0.215 | 1.046247731 | 0.289309 | 2.96148E-07 | 0.000153922 |
| 0.225 | 0.838934386 | 0.259065 | 2.00955E-06 | 0.000400954 |
| 0.235 | 0.678506133 | 0.232982 | 7.44651E-08 | 7.7183E-05 |
| 0.245 | 0.553201129 | 0.210371 | 4.3349E-09 | 1.86224E-05 |
| 0.255 | 0.454461002 | 0.190675 | 7.23366E-09 | 2.4056E-05 |

From the result obtained above, the graphs of heave motion spectrum and heave response were plotted. Figure 4.5 is the graph of heave motion spectrum. It shows that the spectrum is fluctuated randomly with maximum value of 0.0065 m^2 .

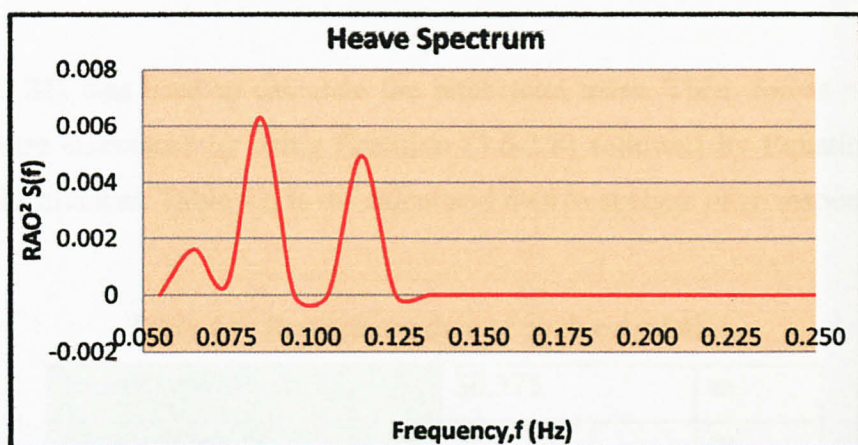


Figure 4.5: Heave Motion Spectrum

The graph of heave response is next plotted in Figure 4.6. From the graph, the maximum heave response is 0.028 m.

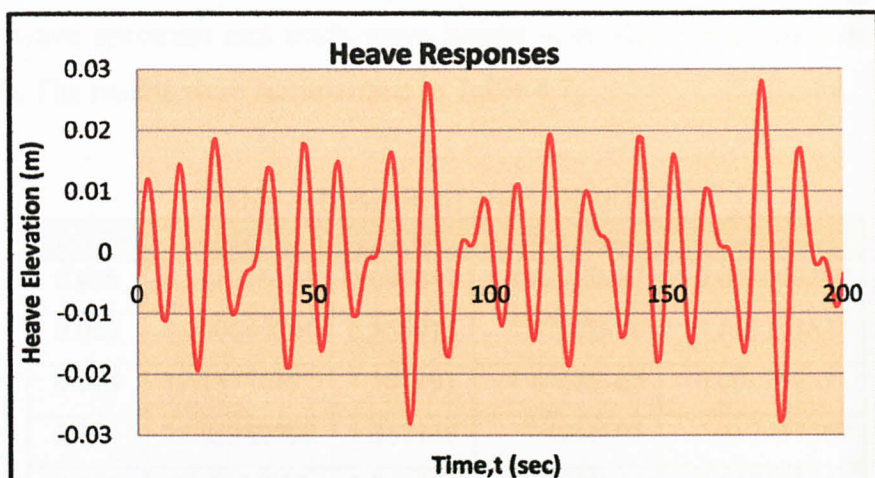


Figure 4.6: Heave Responses

4.1.5 Pitch Calculation

Equation (3.24) was used to calculate the pitch total mass. Then, forces acted on the structure were calculated by using Equation (3.6-3.8) followed by Equation (3.25) to determine its moment. Table 4.6 is the calculated data to analyze pitch response.

Table 4.6: Preliminary data of pitch calculation.

| | | |
|---------------------------|-------------|-----|
| Radius of gyration, R_g | 30.375 | m |
| Centre of gravity, C_g | 3 | m |
| Total pitch mass of TLP | 70495332025 | kg |
| Pitch stiffness | 2.71782E+11 | N/m |

Then, the wave spectrum and pitch wave height were determined by using Equation (3.26-3.27). The results were summarized in Table 4.7;

Table 4.7: Result of pitch calculation

| f | $S(f)$ | $H(f)$ | $RAO^2.S(f)$ | Pitch $H(f)$ |
|-------|-------------|----------|--------------|--------------|
| 0.055 | 0.111016121 | 0.094241 | 3.6297E-07 | 0.017040389 |
| 0.065 | 4.060044004 | 0.569915 | 4.9792E-06 | 0.063113674 |
| 0.075 | 15.15776892 | 1.101191 | 4.8958E-08 | 0.006258331 |
| 0.085 | 22.85382792 | 1.352149 | 7.426E-05 | 0.2437369 |
| 0.095 | 23.2376275 | 1.363455 | 5.7109E-06 | 0.067592067 |
| 0.105 | 19.73879336 | 1.256624 | 1.9661E-05 | 0.125414226 |
| 0.115 | 15.43543965 | 1.111231 | 3.0003E-05 | 0.154926085 |
| 0.125 | 11.64370992 | 0.965141 | 2.1771E-08 | 0.004173309 |
| 0.135 | 8.673947052 | 0.833016 | 7.6937E-07 | 0.024809154 |
| 0.145 | 6.458187473 | 0.718787 | 8.5106E-10 | 0.000825134 |
| 0.155 | 4.835541436 | 0.621967 | 1.9609E-08 | 0.003960737 |
| 0.165 | 3.652119978 | 0.540527 | 1.9037E-07 | 0.012340885 |
| 0.175 | 2.786155703 | 0.472115 | 1.4082E-07 | 0.010613843 |
| 0.185 | 2.147934628 | 0.41453 | 1.3546E-08 | 0.003291969 |
| 0.195 | 1.673278457 | 0.365872 | 3.3732E-08 | 0.005194786 |
| 0.205 | 1.316758148 | 0.324562 | 2.4433E-08 | 0.004421119 |
| 0.215 | 1.046247731 | 0.289309 | 1.2424E-08 | 0.00315267 |
| 0.225 | 0.838934386 | 0.259065 | 1.8243E-09 | 0.00120808 |
| 0.235 | 0.678506133 | 0.232982 | 2.2634E-10 | 0.000425522 |
| 0.245 | 0.553201129 | 0.210371 | 8.4428E-10 | 0.00082184 |
| 0.255 | 0.454461002 | 0.190675 | 5.8398E-11 | 0.000216144 |

The graphs of pitch spectrum and pitch response were plotted in Figure 4.7 and Figure 4.8 respectively.

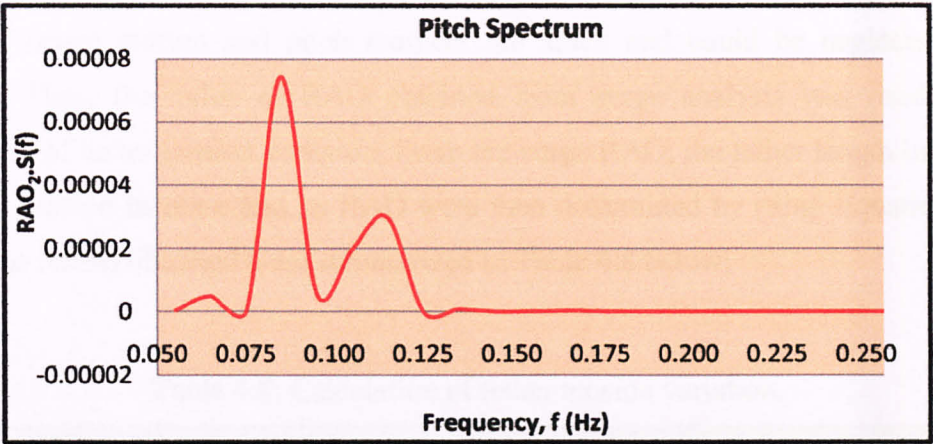


Figure 4.7: Pitch Motion Spectrum

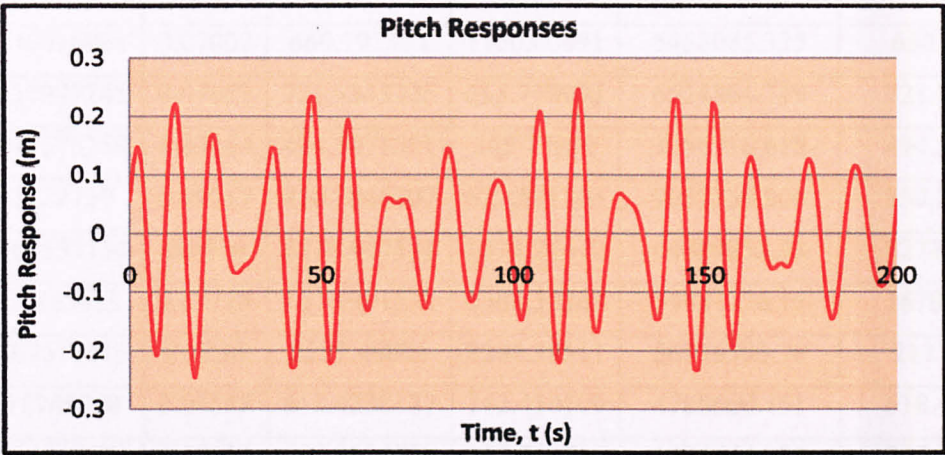


Figure 4.8: Pitch Response

Figure 4.8 shows the excursion of wave height due to the pitch motion. the maximum pitch response is 0.245 rad or 7.03°.

4.1.6 Tether Tension Variation of TLP

Tension of tether is assumed to be totally due to the surge motion. This is because, the effect of heave motion and pitch moment are small and could be neglected in the analysis. Thus, the value of RAO obtained from surge analysis was used for the calculation of tether tension variation. From the surge RAO; the tether length increment, stiffness, tension increase and its RAO were then determined by using Equation (3.28-3.30). The results obtained were summarized in Table 4.8 below;

Table 4.8: Calculation of tether tension variation.

| f (Hz) | RAO_{Surge} | Δ (m) | Increase in Tension (kN/m) | $RAO_{Tension}$ (kN) | $RAO_{Tension}^2 \cdot S(f)$ | Tether Tension H(f) |
|-------------|---------------|--------------|----------------------------------|-------------------------|------------------------------|------------------------|
| 0.055 | 0.917691161 | 0.0432 | 407.4056999 | 4327.05163 | 2074742.554 | 407.4056999 |
| 0.065 | 0.246016961 | 0.07007 | 660.791364 | 1160.00691 | 5458065.335 | 660.791364 |
| 0.075 | 0.139077245 | 0.07655 | 721.9343305 | 655.770095 | 6514864.719 | 721.9343305 |
| 0.085 | 0.077575258 | 0.05244 | 494.5071581 | 365.77899 | 3056716.618 | 494.5071581 |
| 0.095 | 0.1322739 | 0.09017 | 850.2865307 | 623.691303 | 9037339.804 | 850.2865307 |
| 0.105 | 0.384557154 | 0.2416 | 2278.407378 | 1813.24472 | 64889252.23 | 2278.407378 |
| 0.115 | 0.31883453 | 0.17714 | 1670.491572 | 1503.35268 | 34881776.15 | 1670.491572 |
| 0.125 | 0.467511115 | 0.2256 | 2127.46805 | 2204.38511 | 56576503.78 | 2127.46805 |
| 0.135 | 0.15745208 | 0.06558 | 618.4238127 | 742.410199 | 4780600.151 | 618.4238127 |
| 0.145 | 0.084347003 | 0.03031 | 285.8624818 | 397.708785 | 1021466.981 | 285.8624818 |
| 0.155 | 0.037130389 | 0.01155 | 108.8895459 | 175.07536 | 148211.6651 | 108.8895459 |
| 0.165 | 0.248851515 | 0.06725 | 634.2322979 | 1173.37226 | 5028132.597 | 634.2322979 |
| 0.175 | 0.289261177 | 0.06828 | 643.9163181 | 1363.90989 | 5182852.809 | 643.9163181 |
| 0.185 | 0.030088245 | 0.00624 | 58.80912992 | 141.870591 | 43231.42202 | 58.80912992 |
| 0.195 | 0.020253003 | 0.0037 | 34.93908305 | 95.4959493 | 15259.24405 | 34.93908305 |
| 0.205 | 0.086916574 | 0.0141 | 133.0129848 | 409.824697 | 221155.6764 | 133.0129848 |
| 0.215 | 0.212787735 | 0.03078 | 290.2703344 | 1003.32613 | 1053210.838 | 290.2703344 |
| 0.225 | 0.118072504 | 0.01529 | 144.2287554 | 556.729589 | 260024.1734 | 144.2287554 |

| | | | | | | |
|-------|-------------|---------|-------------|------------|-------------|-------------|
| 0.235 | 0.005717912 | 0.00067 | 6.281359455 | 26.9608124 | 493.1934575 | 6.281359455 |
| 0.245 | 0.100648852 | 0.01059 | 99.83661614 | 474.574451 | 124591.874 | 99.83661614 |
| 0.255 | 3.61474E-05 | 3.4E-06 | 0.032498628 | 0.17044042 | 0.01320201 | 0.032498628 |

From the result in Table 4.8, the graph of tether tension spectrum and its variation were plotted in Figure 4.9 and Figure 4.10 as below;

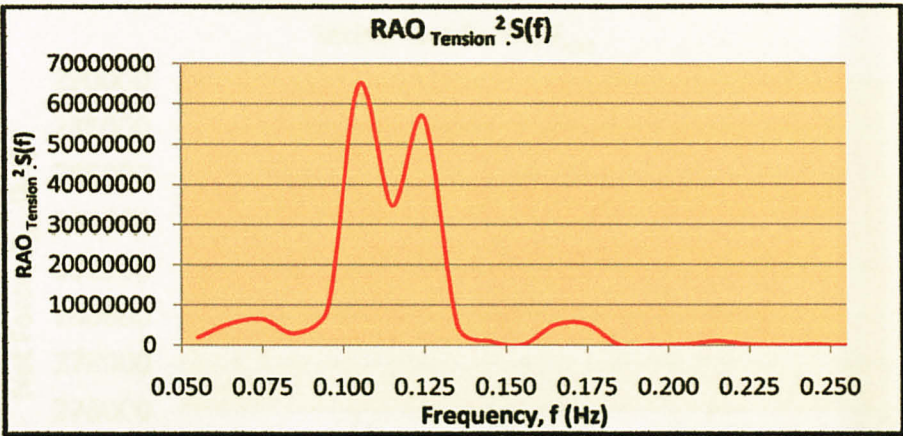


Figure 4.9: Tether tension Spectrum

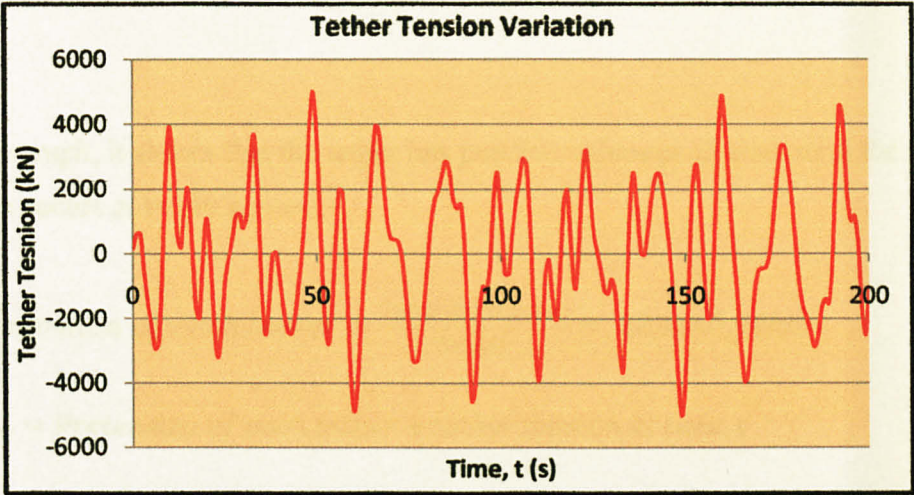


Figure 4.10: Tether tension variation.

From Figure 4.10, the minimum and maximum tether tension is ± 5004 kN. To keep the tether in tension, the net forces, F_{net} acting along the tether length must be always positive.

Net forces, F_{net} are determined by adding up the tether pretension with the tether tension at each time. The result obtained is plotted as in Figure 4.11 below;

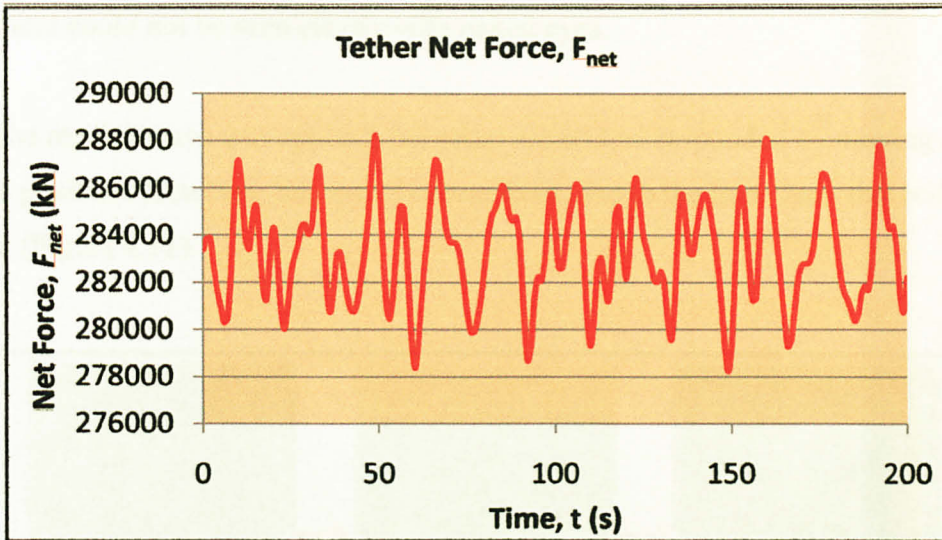


Figure 4.11: Tether Net Force, F_{net}

From this graph, it shows that the tether has positive values at all time with the minimum net forces occurs at $t=149$ second.

$$\text{Pretension of each tether} = \frac{\text{Total Pretension}}{\text{tether}} = 283240.98 \text{ kN}$$

$$F_{\text{net}} = \text{Pretension of each tether} + \text{tether tension at time, } t$$

$$F_{\text{net}} = 283240.98 \text{ kN} - 5004 \text{ kN} = +278237 \text{ kN}$$

4.2 Model Experiment Analysis

During the experiment, the surge responses (x-direction) had been recorded. The heave responses could not be recorded since its motion is very small and almost negligible. The iron chains that are kept in tension had caused the heave responses in the experiment could not be seen clearly with naked eyes.

When the regular wave was applied, the setup model had responded by moving from its original position. However, the model moved back due to the iron chain that restrains its motion. (Figure 4.11)

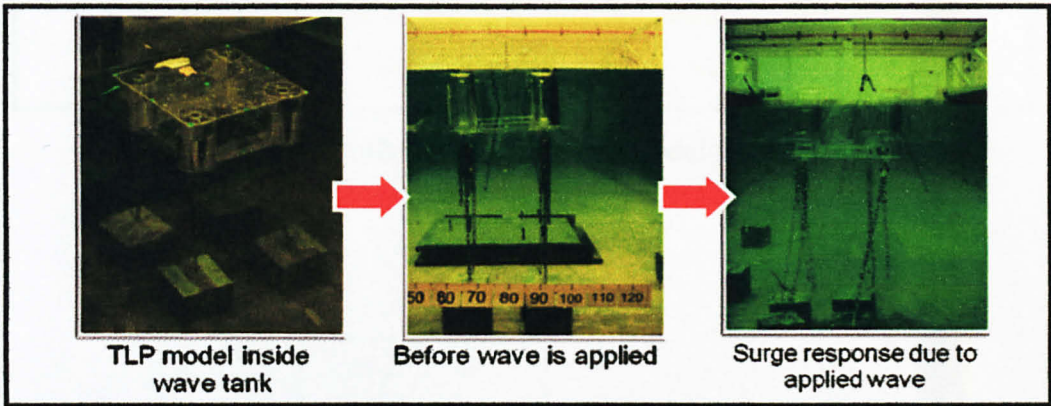


Figure 4.11: The response of setup model in the wave tank

The result of the experiment were recorded and summarized in the Table 4.9. The result was plotted in the graph as Figure 4.12.

Table 4.9: Result of surge motion of model testing

| | <i>f</i> , H | Surge Motion |
|---|-----------------|--------------|
| 1 | <i>f</i> = 1 Hz | ± 6 cm |

| | | |
|---|--|---------------------|
| | $H = 0.1 \text{ m}$ | |
| 2 | $f = 0.5 \text{ Hz}$ $H = 0.05 \text{ m}$ | $\pm 10 \text{ cm}$ |
| 3 | $f = 1 \text{ Hz}$ $H = 0.05 \text{ m}$ | $\pm 4 \text{ cm}$ |

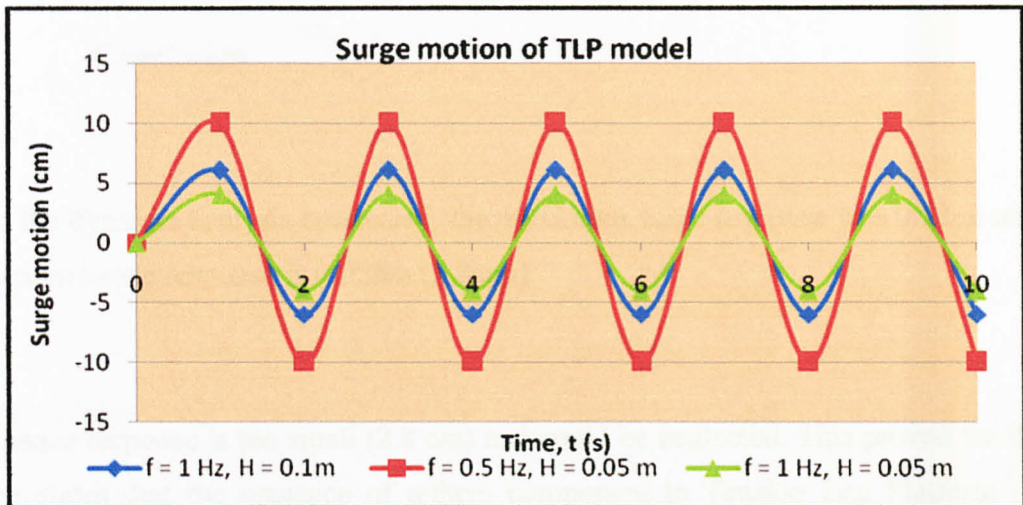


Figure 4.12: Surge motion of model testing

CHAPTER 5

CONCLUSION & RECOMMENDATION

5.1 Conclusion

From the dynamic analysis conducted, the maximum surge response was 0.52 m and the maximum heave response is 0.028m (2.8 cm).

The heave response is too small (2.8 cm) and could be neglected. This proved the theory which states that the presence of tethers component in Tension Leg Platform (TLP) restrains the structure from moving vertically. Since the wave forces and heave response are acting on the contradicting plane, the impact on the structure would be lesser.

From pitch response analysis, the structure would be tilted by 7.03 degree due to the moment produced. Thus, the structure should be designed such that, it would not oscillate more than 7.03 degree unless the structure would just collapsed. The effect of pitch could be decreased by lowering its centre of gravity, C_g thus, increasing its stability.

The analysis of tether tension variation proves that the net tension force of tether is always having positive value. Each tether would have the net tension force, F_{net} of at least 278.237 MN along the tether.

From the experimental analysis, the lesser wave frequency ($f = 0.5$ Hz instead of $f = 1$ Hz) has larger impact on the model.

5.2 Recommendation

Motion responses of conventional TLP should be compared with various types of TLP such as SeaStar TLP, Moses TLP or Mini-TLP. Thus, the TLPs with less response could be observed and compared.

Besides that, a deeper research could be conducted to determine the ration of surge and heave motion. Thus, the relationship between both motions could be identified and further discussed.

TLP model should be fabricated with heavier type of material, so that the model should be ensure to have less motion during model testing is done. Special apparatus/instrument should be installed to obtain accurate result.

To compare the accuracy of the result of dynamic analysis, advanced software like SACS should be used.

REFERENCES

- S. K. Chakrabati 2001, *Hydrodynamic of Offshore Structures*, USA, WIT Press.
- Chakrabarti Subrata - Handbook of Offshore Engineering, Volume 1&2.
- Lindsey Wilhoit and Chad Supan of Mustang Engineering, 2007, Worldwide Survey of TLPs, TLWP, www.mustangeng.com.
- Chandrasekaran and A. K. Jain 2000, *Dynamic Behaviour of Square and Triangular Offshore Tension Leg Platforms under Regular wave Loads*, Indian Institute of Technology, Delhi, India.
- N.A. Siddiqui, Suhail Ahmad 2001, *Fatigue and Fracture Reliability of TLP Tethers under Random Loading*, Aligarh Muslim University and Department of Applied Mechanics, IIT Delhi.
- John W. Chianis, Phillip B. Poll and ABB Lummus Global Oil & Gas- America Houston Offshore Petroleum Operation, *New concepts extend dry-tree production into deeper water*, Oil & Gas Journal Special May 3, 1999.
- M. A. Brogan, Massachusetts Institute of Technology; K. S. Wasserman, MIT, *Tension Leg Platform Design Optimization for Vortex Induced Vibration*
- Hiroshi Iwasaki 1981, *A Preliminary Design Study of the Tension Leg Platform*, Master of Science in Ocean Engineering, Massachusetts Institute of Technology.

- Alberto Morandi, Diego Martinez and Charles Smith, *Statistics of TLP Tendon Tension Behaviour during Hurricane Lili*, 23rd International Conference on Offshore Mechanics and Arctic Engineering, 2004.
- Hsien Hua Lee, Pei-Wen Wang, Chung-Pan Lee, 1997, *Dragged Surge Motion of Tension Leg Platforms and Strained Elastic Tethers*, National Sun Yat-sen University, Kaohsiung, Taiwan.
- Alberto Morandi, Diego Martinez, Charles Smith, 2004, “*Statistics of TLP Tendon Tension Behaviour during Hurricane Lili*”, 23rd International Conference on Offshore Mechanics and Arctic Engineering.
- Ximenes, M.C.C., Mansour, A.E., 1991, “*Fatigue system reliability of TLP tendons including inspection updating*,” Proc. of the 10th International Conference on Offshore Mechanics and Arctic Engineering, OMAE’91.
- Pieter Aalberts and Radboud van Dijk, Weizhong Zheng, 2008, “*Effect of Hurricanes On The Cumulative Fatigue Life Consumption of A Gom TLP*”, Proceedings of the 27th International Conference on Offshore Mechanics and Arctic Engineering.
- S. Botker, F. Mo, and H. Hannus, “*Dragged Surge Motion of Tension Leg Platforms And Strained Elastic Tethers*,” Offshore Technology Conference, Houston, TX, USA, 2005.
- Hsien Hua Lee and Pei-Wen Wang, “*Surge, Motion of Tension Leg Platform with Underwater Net Systems*,” Proceedings of the Ninth (1999) International Offshore and Polar Engineering Conference.
- Pallanich, J. (2008, January). Extending the TLP brand. *Offshore*, 38-39.

Patel, M.H., Witz, J.A., (1991). *Compliant Offshore Structures*. Great Britain:
Butterworth-Heinemann